Available online at www.sciencedirect.com
ScienceDirect
Journal of Hazardous Materials 151 (2008) 710–719
Journal of Hazardous Materials
www.elsevier.com/locate/jhazmat

Preparation and sorption properties of materials from paper sludge

M. Hojamberdiev [1], Y. Kameshima, A. Nakajima, K. Okada *, Z. Kadirova [2]

Department of Metallurgy and Ceramics Science, Tokyo Institute of Technology, O-okayama, Meguro, Tokyo 152-8552, Japan

Received 19 January 2007; received in revised form 31 May 2007; accepted 13 June 2007
Available online 20 June 2007

Abstract

Three materials were prepared from paper sludge (PS) using different treatment processes and their sorption abilities for phosphate and methylene blue (MB) were determined. The samples were a powder sample prepared by heating PS in air (sample C), a pellet prepared by grinding, forming and heating PS in air (sample G) and a powder prepared by physical activation of PS in flowing wet nitrogen (sample A). The three samples were heated at 600–900 °C for 6 h. On heating at 700–800 °C, the organic fibers, limestone ($CaCO_3$), kaolinite ($Al_2Si_2O_5(OH)_4$) and talc ($Mg_3Si_4O_{10}(OH)_2$) in the original PS were converted to amorphous CaO–Al_2O_3–SiO_2 (CAS) and talc in sample C, while CAS was formed in sample G and activated carbon, CAS and talc was formed in sample A. On heating at 900 °C the CAS converted to gehlenite ($Ca_2Al_2SiO_7$) and anorthite ($CaAl_2Si_2O_8$). The specific surface areas (S_{BET}) of the three samples achieved maximum values of 23, 37 and 70 m^2/g upon heating at 700, 600 and 600 °C, respectively. The S_{BET} value of the activated sample A was distinctly lower than usually reported for activated carbon. The samples C, G and A achieved maximum phosphate sorption capacities of 2.04, 1.38 and 1.70 mmol/g, calculated from the Langmuir model, upon heating at 700, 700 and 800 °C, respectively. The maximum sorption capacity for phosphate in sample C is attributed to the sorption by CAS, namely, adsorption on the alumina component and precipitation as Ca-phosphates. The MB multifunctional sorption capacity of sample A was 0.11 mmol/g. The phosphate and MB sorption rates show better correlation with a pseudo-second order model than with other models.

Keywords: Paper sludge; Simultaneous sorption; Physical activation; Mechanical grinding; Calcination; Phosphate ion; Methylene blue

1. Introduction

Rapidly increasing environmental contamination by solid wastes arising from progressive industrialization is an important environmental problem. The paper industry is of great environmental importance due to the quantity of paper sludge generated, and its disposal. Paper sludge generated by the paper industry is generally composed of organic fibers (cellulose, hemicellulose and/or lignin), inorganic fillers and coating materials such as kaolinite ($Al_2Si_2O_5(OH)_4$), limestone ($CaCO_3$) and talc ($Mg_3Si_4O_{10}(OH)_2$). Paper sludge is usually disposed of in open dumps or in landfills, recycled as compost or incinerated for energy recovery in the manufacturing process. However, reduction of available landfill space increasing costs of land disposal of waste in industrial countries necessitates other means for the disposal of waste paper sludge. An economically valuable solution to this problem should include utilization of the waste materials as new products for other applications rather than disposal in a landfill.

Paper sludge can be used to improve soil properties because it has a high carbon content, providing beneficial effects on soils that are deficient in organic matter. Paper sludge has been used in agriculture, as a soil improver and fertilizer [1,2]. Tay and Show [3] have examined the use of incinerated paper sludge ash as a building material. A maximum of 5% of waste paper sludge can be used as an additive in concrete [4]. Furthermore, paper sludge can be economically and efficiently converted into various materials such as highly reactive metakaolin which can be used as starting materials for porous ceramics [5], zeolites with high cation exchange properties [6], coating pigment and papermaking fillers [7], polymer composites [8], glass-ceramics [9], activated carbons [10], etc. Another possible effective use for paper sludge ash is in the preparation of low cost sorbents for water purification, using steam and/or calcination treatments.

* Corresponding author. Tel.: +81 3 5734 2524; fax: +81 3 5734 3355.
E-mail address: kokada@ceram.titech.ac.jp (K. Okada).
[1] Present address: Tashkent Institute of Chemical Technology, 32, Navoi Street, Tashkent 700011, Uzbekistan.
[2] Present address: Institute of General and Inorganic Chemistry Academy of Sciences, 77a, Abdullaev Street, Tashkent 700170, Uzbekistan.

0304-3894/$ – see front matter © 2007 Elsevier B.V. All rights reserved.
doi:10.1016/j.jhazmat.2007.06.058

Amorphous $CaO–Al_2O_3–SiO_2$ prepared from solid-state reaction of kaolinite and $CaCO_3$ by calcining paper sludge at 500–1000 °C showed excellent sorption properties for various heavy metals, and eutrophication related phosphate and ammonium ions [11]. Al-containing $CaO–SiO_2–H_2O$ phases have been synthesized by hydrothermal treatment of mixtures of paper sludge ash with various silica and calcium sources for the simultaneous uptake of eutrophication related ammonium and phosphate ions [12]. Zeolite Na-P1 has been synthesized from paper sludge ash by low-temperature hydrothermal treatment (at 90 °C). The resulting Na-P1 exhibits a high cation exchange capacity for NH_4^+ and considerable ability to sorb phosphate by precipitation of calcium phosphate without the addition of extra calcium; this is preferable for water purification applications [6]. According to Khalili et al. [10], paper sludge can successfully be converted into activated carbon with $S_{BET} > 1000\ m^2/g$ by chemical activation using $ZnCl_2$.

Thus, low cost sorbents can be produced from many raw materials such as industrial and agriculture wastes. Recycling and re-using of wastes have energy efficient, environmentally friendly and cost-effective advantages. This study investigates the preparation of low cost, harmless and high efficiency porous materials from paper sludge by calcination, grinding and/or physical activation processes. The aim is to improve the simultaneous removal of harmful inorganic and organic ions from water and to find original ways of utilizing of waste paper sludge. In this paper, phosphate ion was chosen as a model adsorbate for harmful inorganic ion because it is one of the important target ions for eutrophication and also shows analogy with highly toxic arsenate ion. On the other hand, methylene blue was chosen as a model adsorbate for harmful organic dye because it is generally used for evaluation of sorption ability of organic ions.

2. Experimental

2.1. Sample preparation

Paper sludge (PS) from the Fuji Paper Making Union, Fuji, Japan was used as the starting material. The PS was dried at 110 °C for 24 h and treated by the following methods to prepare the samples:

2.1.1. Sample C (calcination)

The PS was calcined in an alumina crucible at 600–900 °C for 6 h in air.

2.1.2. Sample G (mechanochemical grinding)

The PS was crushed using an alumina mortar and pestle, then, dry-ground in a planetary ball mill (LAPO-1, Ito Seisakusho Ltd., Japan) using an alumina pot (80 mL) with 300 alumina balls (5 mm Ø) at 300 rpm for 12 h with a ball/sample mass ratio of 15:1. The ground powder was uniaxially pressed into a pellet at 100 MPa and heated at 600–900 °C for 6 h. The heating rate was set to 1 °C/min up to 300 °C to avoid breaking the pellet due to abrupt ignition of the organic fibers. After fiber burnout, the heating rate was increased to 10 °C/min up to the prescribed temperature. The bulk density, water adsorption, apparent porosity and total shrinkage of pellet samples were measured according to the ASTM Standard Test Method [13,14].

2.1.3. Sample A (physical activation)

The samples were prepared by physical activation of PS using wet N_2. The PS was heated at 600–900 °C in a Ni crucible at a heating rate of 10 °C/min in flowing dry N_2 (0.5 L/min) then maintained at the holding temperature in flowing wet N_2 containing 20 mol% steam. The sample was then cooled in flowing dry N_2 at 10 °C/min.

2.2. Sorption experiment

Sorption experiments were performed on the three types of sample under the following conditions: sample/solution ratio: 0.1 g/50 mL, reaction time: 24 h, reaction temperature: room temperature, initial concentration of phosphate ($NH_4H_2PO_4$): 1–10 mmol/L, initial concentration of methylene blue (MB, $C_{16}H_{18}N_3SCl{\cdot}3H_2O$): 0.001–0.25 mmol/L. The pH values were measured before putting samples into solution (initial pH) and after the reaction (final pH) using a pH meter (HM-20J, TOA DKK, Japan). After the sorption experiments, the solid samples were separated from the solution by filtration, washed with distilled water and dried at 110 °C overnight. The concentration of phosphate ion was measured by an ion chromatograph (IA-200, DKK TAO, Japan). The concentration of MB was determined using a UV–vis spectrophotometer (V-630 IRM, JASCO Engineering Co., Japan) at a wavelength of 665 nm.

2.3. Characterization

The chemical compositions of the samples were analyzed by X-ray fluorescence (RIX2000, Rigaku, Japan). The crystalline phases in the samples were identified by powder X-ray diffraction with monochromated Cu Kα radiation (LabX XRD-6100, Shimadzu, Japan). Differential thermal analysis (DTA)/thermogravimetry (TG) (TG-8120, Rigaku, Japan) was carried out in the temperature range 20–1000 °C at a heating rate of 10 °C/min in flowing air. The microstructure of these samples was observed by scanning electron microscopy (JSM-5310, JEOL, Japan) at an accelerating voltage of 20 kV after Pt coating. The specific surface area (S_{BET}), pore size distribution and total pore volume were obtained from N_2 adsorption-desorption isotherms at 77 K (Autosorb-1, Quanta Chrome, USA), on samples preheated at 120 °C for 20 h in vacuo. The S_{BET} values were calculated by the Brauner, Emmett and Teller (BET) method and the pore size distribution was determined by the Barrett, Joyner and Halenda (BJH) method using the desorption isotherms.

3. Results and discussion

3.1. Characterization of the starting material

The chemical composition of the PS is listed in Table 1. The PS contains C in the form of organic fibers, and inorganic components, predominantly SiO_2, CaO and Al_2O_3. The XRD

Table 1
Chemical compositions (mass%) of materials from paper sludge

Sample	C	SiO_2	Al_2O_3	CaO	MgO	Fe_2O_3	TiO_2	K_2O	P_2O_5	SO_3	Cl
Paper sludge	52.2	16.1	13.6	14.2	2.8	0.4	0.6	0.1	0.4	0.3	0.2
C700	5.5	31.1	27.2	26.2	6.2	0.7	1.5	0.2	0.8	0.4	0.1
G700	5.3	32.7	27.0	25.5	5.9	0.7	1.3	0.1	0.8	0.5	0.1
A800	21.8	26.4	23.4	20.7	4.9	0.5	1.1	0.1	0.7	0.2	0.1

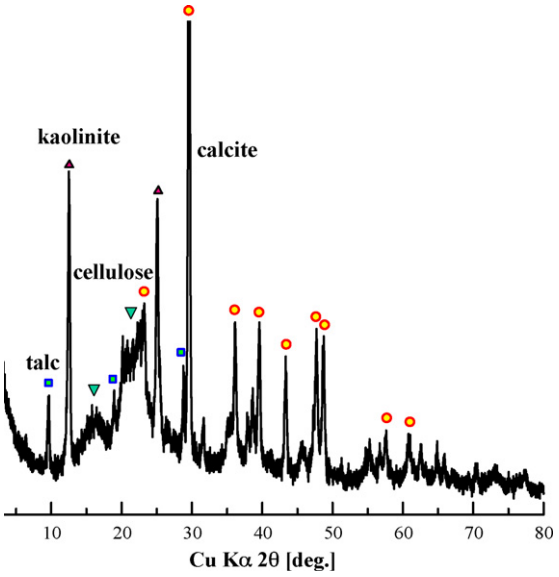

Fig. 1. XRD pattern of the paper sludge. *Key*: ▽ = cellulose, ◯ = calcite, △ = kaolinite and □ = talc.

pattern of the PS (Fig. 1) shows that the main crystalline constituents are cellulose (with relatively broad peaks due to the low crystallinity of the fibers) and calcite, kaolinite and talc (the filler and/or coating components of the paper). The amount of talc is, however, not high considered from the content of MgO (2.8 mass%) in the PS in Table 1. The DTA and TG curves of the PS are shown in Fig. 2. The DTA curve shows an endothermic peak at 707 °C and three exothermic peaks at 246° (weak), 340° (strong) and 410 °C (strong). Corresponding to these peaks, the TG curve shows three step weight losses of 4.3 mass% by 250 °C, 43.0 mass% between 250 and 600 °C and 7.0 mass% between 600 and 710 °C. The distinct exothermic peaks at 340 and 410 °C with large associated weight losses correspond to the burning of the organic fibers. By contrast, the endothermic peak and weight loss at about 700 °C is attributed to the decarbonation of $CaCO_3$. The endothermic peak at 500–600 °C associated with the dehydroxylation of kaolinite did not appear in the DTA curve, probably because the dehydroxylation temperature was depressed by the burning of the organic fibers.

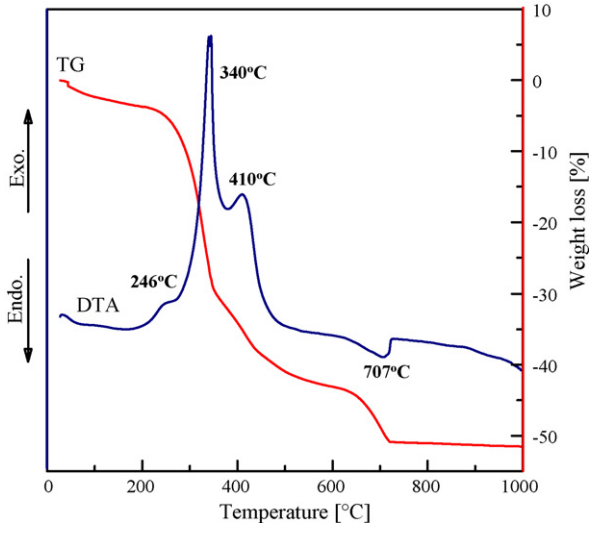

Fig. 2. DTA and TG curves of the paper sludge.

The SEM microphotograph of PS (Fig. 3) shows an agglomerated texture of organic fibers together with fine particles of kaolinite, talc and calcite [15]. Since the organic fibers in the PS had been recycled several times, some were broken to resemble powder, with very small numbers maintaining the original fiber shape.

3.2. Characterization of the samples

The XRD patterns of samples C, G and A heated at various temperatures are shown in Fig. 4a–c, respectively. The XRD patterns of the samples C and A show similar changes on heating, but the effect on sample G of heating is different. The peaks corresponding to kaolinite and talc disappeared in the ground PS sample, resulting in the highly amorphized XRD patterns in the heated G-series samples. None of the XRD patterns of the heated samples show peaks of kaolinite because of its conversion to amorphous metakaolinite. By contrast, a new peak at $2\theta = 6.3°$ appeared in samples C and A heated at 600 and 700 °C [16]. The *d* spacing of this peak (1.4 nm) suggests that it may be due to chlorite, but since the formation of this phase would not be expected on heating in an open atmosphere, the origin of this reflection requires further examination. The peak at $2\theta = 25.3°$, assigned to anatase, occurs in PS as an accessory phase, and becomes clearer upon heating. The peaks assigned to calcite disappear upon thermal decarbonation at 700 °C in sample C and at 800 °C in sample A, but at a much lower temperature (<600 °C) in sample G. Thus, the decarbonation temperature of the PS strongly depends on the sample treatment, i.e. it is lowered by mechanochemical grinding but increased by heating in a wet N_2 atmosphere. Enhancement of various reactions by mechanochemical grinding is generally known owing to the increase of surfaces and introduction of stress [17]. By contrast, the decarbonation is suppressed due to the lowering of oxygen partial pressure in the N_2 atmosphere. Talc is retained in samples C and A up to 800 °C, indicating its greater thermal stability than kaolinite and calcite [18]. The amount of amorphous

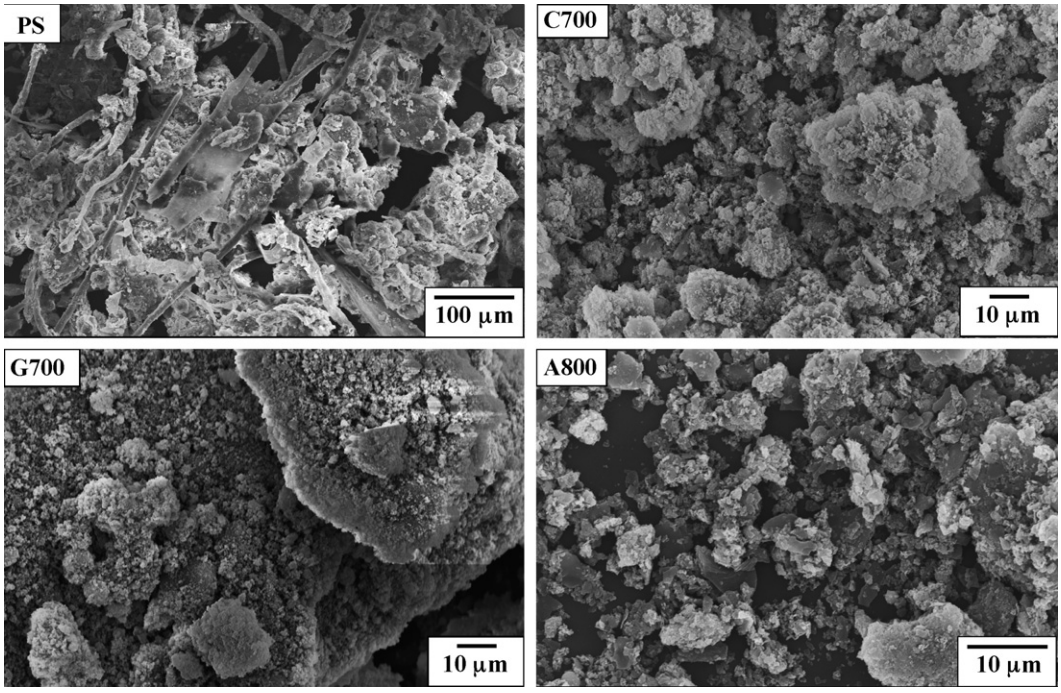

Fig. 3. SEM photographs of the paper sludge (PS), C700, G700 and A800 samples.

$CaO–Al_2O_3–SiO_2$ (CAS), appearing as a halo at $2\theta = 25–30°$, increases in the order sample A < sample C < sample G. Above 800 °C, the XRD patterns of the three samples show the formation of new phases such as gehlenite ($Ca_2Al_2SiO_7$) and anorthite ($CaAl_2Si_2O_8$) by crystallization of CAS [18].

Changes in the S_{BET} values of the three samples, shown in Fig. 5 as a function of heating temperature, indicate a decrease in the S_{BET} values with increasing temperature. The temperatures giving the highest S_{BET} values were relatively low (700, 600 and 600 °C for samples C, G and A, respectively). The maximum S_{BET} values were the highest in sample A (70 m^2/g) and the lowest in sample C (22 m^2/g). This difference in S_{BET} values between sample G and sample C is attributed to the formation of finer particles by dry milling, which also enhances the formation of amorphous CAS (Fig. 4). A significant increase of S_{BET} by mechanical activation has been reported by Temuujin et al. [19]. The S_{BET} values of sample A prepared by physical activation of PS are clearly lower than those reported for other activated carbons prepared from paper sludge and waste paper using different activation methods [9,15,20]. This may reflect a lower carbon content in the present PS. Presence of activated carbon is indicated from the pore size distribution of the sample A but the amount of adsorption corresponded to the activated carbon seems to be low compared with those synthesized from old newspaper, having much higher S_{BET} (about 1700 m^2/g) by higher carbon content [15]. The main pore sizes formed in the three samples were very similar each other and about 50–60 nm in pore size. They are, therefore, considered to correspond to the spaces formed by agglomeration of small particles.

The SEM images of the heated samples C700, G700 (powdered the pellet) and A800 are shown in Fig. 3. All three samples are similar, consisting of agglomerated fine particles. Sample A800 contains particles with smooth surfaces, which indicate the presence of activated carbon.

One of the purposes of this study is to evaluate the difference in the sorption properties of powder and pellet samples, with a view to their applications as low-cost shaped sorbents. Although shaping can be achieved by uniaxial pressing of both unground (as-received) and ground PS without the addition of a binder, the pellets pressed from unground PS broke during heating due to the burning of the organic fibers, even when heated at a slow heating rate (1 °C/min). By contrast, the pellets from the ground PS retained their shape upon heating at 1 °C/min. The physical properties of the pellet samples heated at various temperatures were determined by the ASTM Standard Test Methods [13,14]. Changes in the bulk density and water absorption are shown in Fig. 6 as a function of heating temperature. The very steep increase in bulk density and decrease of water absorption between 700 and 900 °C indicates that densification occurs in this temperature range. Viscous flow is thought to be the dominant mechanism for this densification because crystallization occurs at 900 °C.

3.3. Sorption properties

The phosphate sorption capacities of the three samples determined qualitatively using a constant initial phosphate concentration of 5 mmol/L are shown in Fig. 7 as a function of the sample heating temperature. The phosphate sorption of samples C and G increases up to 700 °C but decreases above this temperature. In the case of sample A, phosphate sorption gradually increases with increasing activating temperatures up to 800 °C but decreases after this. Thus, the maximum sorption is achieved by heating at 700, 700 and 800 °C in samples C,

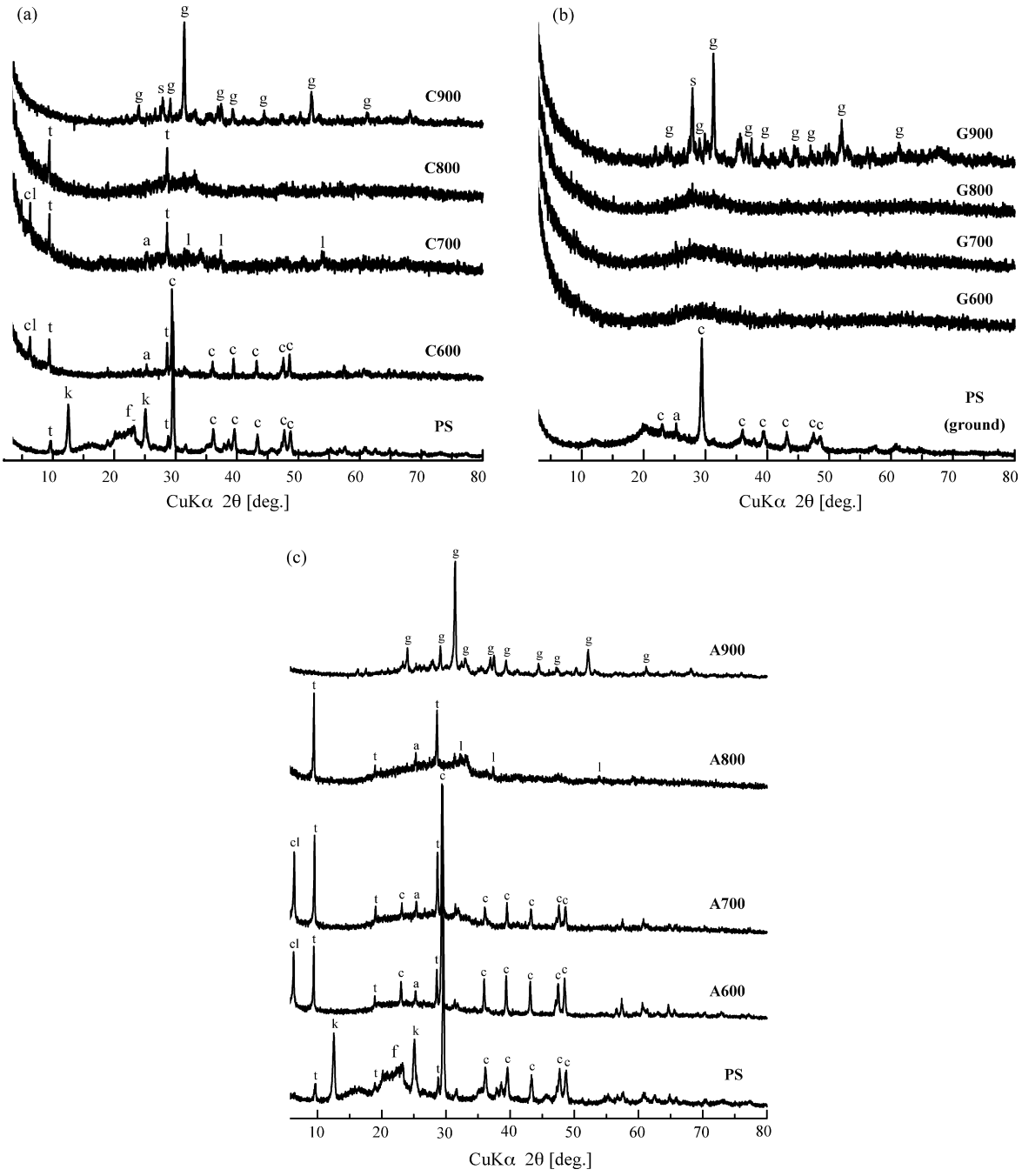

Fig. 4. XRD patterns of sample C (a), G (b) and A (c) heated at various temperatures. *Key*: k = kaolinite, t = talc, c = calcite, f = cellulose, cl = chlorite, a = anatase, g = gehlenite and a = anorthite.

G and A, respectively. It is thought that amorphous CAS was formed by decarbonation of calcite up to 700 °C in the samples C and G, but this occurred in sample A only above 800 °C. The gradual decreases above these temperatures correspond to the decrease in S_{BET} (Fig. 5). Maximum sorption was obtained in samples C700 (1.67 mmol/g), A800 (1.38 mmol/g) and G700 (0.87 mmol/g). The mechanism of phosphate sorption onto these samples can be explained in terms of the precipitation of calcium phosphates and adsorption on aluminol groups [11]. Calcined paper sludge (sample C) sorbed more phosphate than the other two samples. Higher sorption in sample correlates with the pH and Ca^{2+} concentration in the reacted solution, indicating the dissolution of a large amount of calcium from the sample and the precipitation of calcium phosphate. It is known that the presence of Ca^{2+} facilitates phosphate retention by precipitation of calcium phosphates on the solid surfaces [11].

Some Mg-containing materials are reported to show good sorption ability for phosphate from wastewater. For example, the following phosphate sorption capacities have been reported: Mg-Mn-layered double hydroxides (0.721 mmol/g) [21], serpentine (0.09 mmol/g) [22] and blast furnace slag (1.87 mmol/g) [23]. Some authors suggest that superficial hydrolysis of MgO and

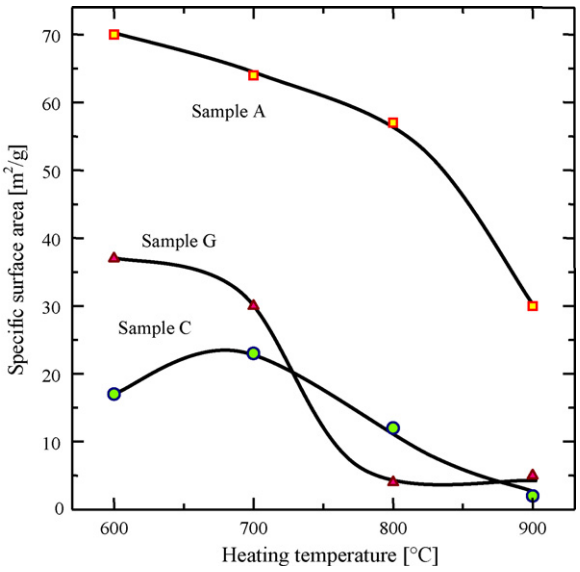

Fig. 5. Change of specific surface areas of the three samples as a function of heating temperature.

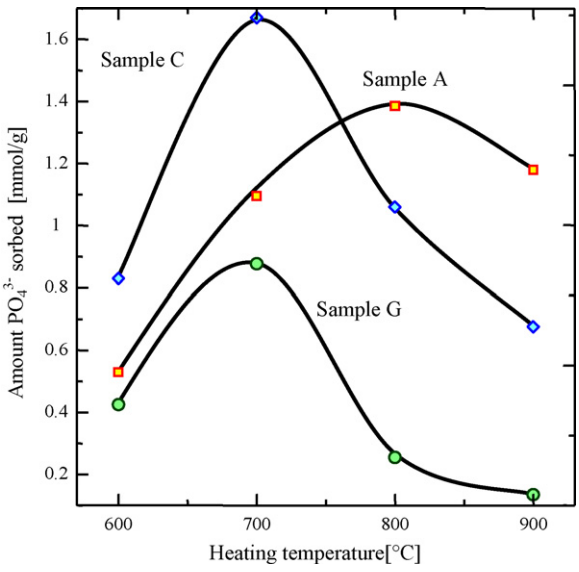

Fig. 7. Change of phosphate sorption by the three samples at an initial concentration of 5 mmol/L as a function of heating temperature.

partial solubilization of the resulting hydroxide results in an exchange of OH^- and Mg^{2+} ions, leading to phosphate fixation at the liquid–solid interface [24]. Thus, an additional opportunity for phosphate sorption might occur in the present samples by virtue of their Mg contents of 4.9–6.2 mass%. Therefore, both Ca^{2+} and Mg^{2+} are thought to contribute to phosphate sorption by the present samples.

The removal of phosphate from solution can be also explained by the Al_2O_3 component in the samples (23–27 mass%). Xie et al. [25] investigated alumina as an adsorbent for removing phosphate from wastewater. A high capacity for phosphate sorption was achieved by acid-treating the alumina. At lower initial phosphate concentrations, phosphate was removed by an adsorption mechanism rather than by precipitation in a coagulation process [26]. At higher initial phosphate concentrations, phosphate is expected to precipitate as $AlPO_4$. Excess alumina was required for complete removal of phosphate (0.03 mmol/g) by alumina alone, especially at lower phosphate concentrations. γ-Al_2O_3 prepared by selective leaching of calcined kaolinite exhibits a higher adsorption capacity (0.33 mmol/g) for phosphate removal from water than other alumina samples [27].

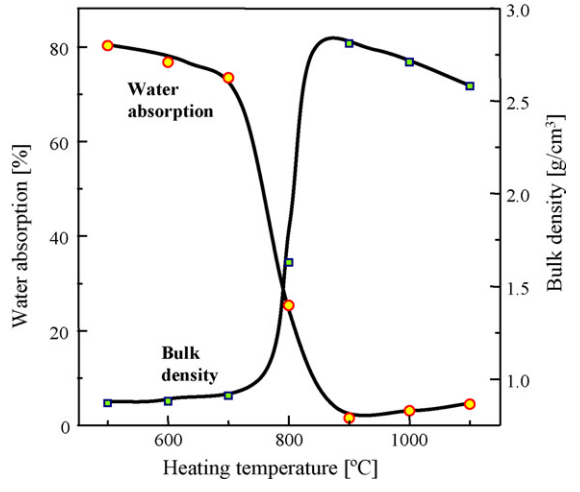

Fig. 6. Change of water absorption and bulk density of sample G as a function of heating temperature.

3.4. Sorption isotherms

The sorption isotherms for phosphate and MB, shown in Fig. 8, indicate a steep increase in the region of low equilibrium concentration but become stable at higher concentrations. Thus, these isotherm data were fitted by the Langmuir (Eq. (1)) [28] and Freundlich (Eq. (2)) [29] equations:

$$\frac{C_e}{Q_e} = \left(\frac{1}{Q_0}\right) C_e + \left(\frac{1}{Q_0 b}\right) \quad (1)$$

$$Q_e = K_F C_e^{1/n} \quad (2)$$

where C_e is the equilibrium concentration (mmol/L), Q_e the amount sorbed at equilibrium (mmol/g), Q_0 the sorption capacity corresponding to monolayer coverage (mmol/g), b the Langmuir constant (L/mmol), and K_F (mmol$^{(1-1/n)}$/(g L$^{1/n}$)) and n are the Freundlich constants. The Langmuir model assumes that sorption occurs on a homogeneous surface by monolayer coverage and the Freundlich model assumes that monolayer sorption occurs on a heterogeneous surface.

The free energy of sorption, ΔG (kJ/mol) can be calculated from the parameter b using the following equation:

$$\Delta G = -RT \ln(b) \quad (3)$$

where R is the gas constant (8.314 kJ/mol K) and T is the temperature (K). The sign of ΔG indicates spontaneity of the reaction, a spontaneous reaction requiring a negative value.

The calculated Langmuir and Freundlich parameters of phosphate and MB sorption are listed in Table 2. In all cases, the resulting correlation coefficients (R^2) show that the Langmuir equation gives a better fit than the Freundlich equation. The

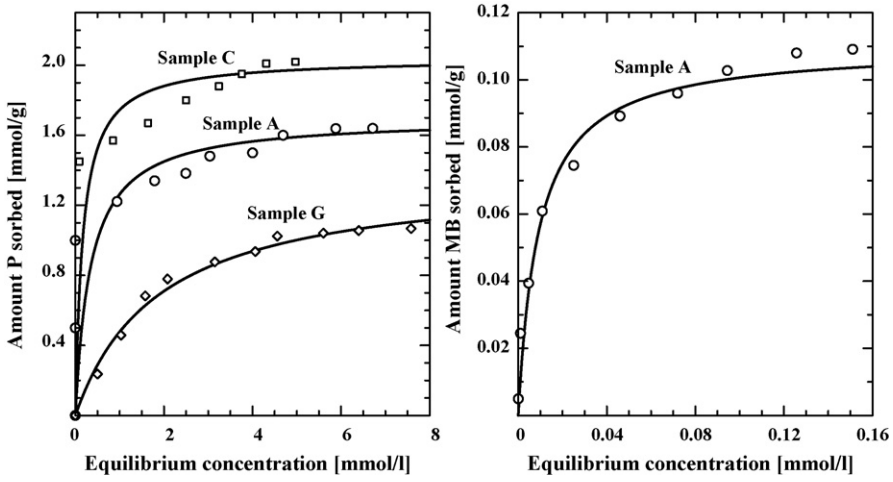

Fig. 8. Phosphate sorption isotherms of the three samples and the MB sorption isotherm of sample A800.

Q_0 values for phosphate sorption increase in the order G700 (1.38 mmol/g) <A800 (1.70 mmol/g) <C700 (2.04 mmol/g). The main difference between samples C and G is their sample shape, i.e., powder or pellet, which results in a large difference in the Q_0 values. On the other hand, the difference in the Q_0 values between samples C and A is attributed to their respective contents of activated carbon and CAS. Since the CAS content of sample C is higher than that in sample A, sorption of phosphate by CAS is higher than by activated carbon. By contrast, the higher activated carbon content of sample A gives it the advantage of high MB sorption, as shown in Fig. 8b. Thus, sample A will simultaneously adsorb both phosphate and organic compounds such as MB.

The ΔG values for phosphate sorption range from −15.5 to −21.5 kJ/mol and for MB sorption −29.0 kJ/mol. These data are in good agreement with the reported data [11,12,18,30]. The negative values indicate that all the sorption reactions in the present samples occur spontaneously.

The saturated phosphate sorption capacities (Q_0) of the present three samples were compared with other reported data, including paper sludge (1.28 mmol/g) [11], refuse paper and plastic fuel (0.95 mmol/g) [30], electric arc furnace steel slag (0.22 mmol/g), serpentine (0.092 mmol/g) [24], aspen wood fiber (0.43 mmol/g) [31], fly ash (0.009 mmol/g) [24], palygorskite (0.88 mmol/g) [32] and Al-containing $CaO–SiO_2–H_2O$ (5.15 mmol/L) [12]. The performance of the present samples is seen to be considerably better than these other sorbents.

The saturated MB sorption capacity (Q_0) of the present sample A800 (0.11 mmol/g) was compared with the following reported data: date pits (0.046 mmol/g) [33], straw (0.052 mmol/g) and rice husk (0.053 mmol/g) [34], lignite coal (0.085 mmol/g) [35], clay (0.016 mmol/g) [36], silica (0.030 mmol/g) [37], pinewood (2.99 mmol/L) [38], paper refuse and plastic fuel (2.07 mmol/g) [30] and waste newspaper (1.04 mmol/g) [39]. Okada et al. [39] have noted that the MB sorption capacity of the aforementioned sorbents depends mainly on the pore size and surface properties of their activated carbon constituents.

3.5. Sorption kinetics

The mechanisms for the removal of phosphate and MB may involve the following four steps [34]: (1) migration of the sorbate from the bulk of the solution to the surface of the sample; (2) diffusion of the sorbate through the boundary layer to the surface of the sorbent; (3) adsorption of the sorbate at an active site on the surface of the sample; (4) intraparticle diffusion of the sorbate into interior pores of the sorbent particles. The boundary layer resistance will be affected by the rate of adsorption and an increase in the contact time, which will reduce the resistance and increase the mobility of the sorbate during adsorption. Since the uptake of sorbates at the active sites of samples is a rapid process, the rate of adsorption is governed mainly by either the rate of liquid phase mass transfer or the rate of intraparticle mass transfer.

Fig. 9 shows the kinetics of phosphate sorption on the present samples C700, A800 and G700 at initial phosphate concentrations of 2 mmol/L, and of MB sorption by sample A800 at

Table 2
Sorption properties of three samples for phosphate and methylene blue (MB)

Sample	Sorbate	Langmuir parameter				Freundlich parameter		
		Q_0 (mmol/g)	b (L/mmol)	R^2	ΔG (kJ/mol)	K_F (mmol$^{(1-1/n)}$/(g L$^{1/n}$))	n	R^2
C700	Phosphate	2.04	5.92	0.9943	−21.50	1.70	11.71	0.8635
G700		1.38	0.53	0.9868	−15.50	0.44	1.90	0.9073
A800		1.70	2.90	0.9935	−19.80	1.22	6.30	0.9767
A800	MB	0.11	122.3	0.9950	−29.00	0.28	2.55	0.9599

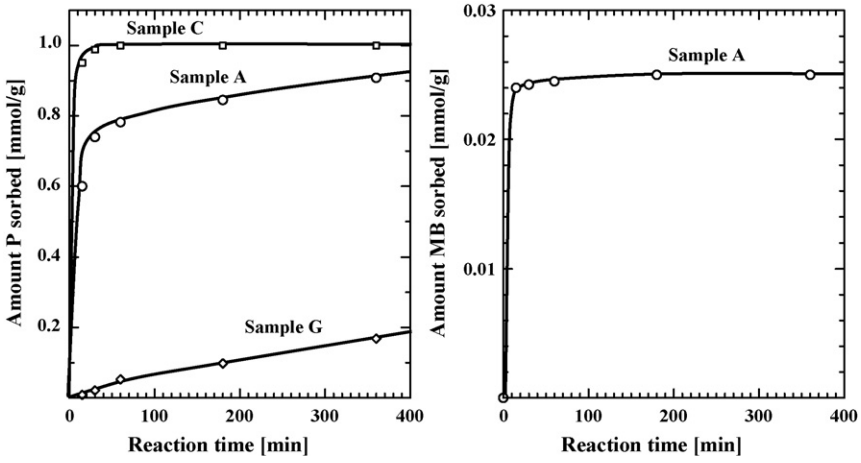

Fig. 9. Change of amount of phosphate sorption by the three samples and the MB sorption by sample A800 as a function of reaction time.

an initial MB concentration of 0.05 mmol/L. The sorption rates were analyzed using a pseudo-first order model (Eq. (4)) [40], a pseudo-second order model (Eq. (5)) [41] and an intraparticle diffusion kinetic model (Eq. (6)) [42].

$$\log(Q_e - Q(t)) = -\left(\frac{k_1}{2.303}\right) t + \log Q_e \quad (4)$$

$$\frac{t}{Q(t)} = \frac{t}{Q_e} + \frac{1}{k_2 Q_e^2} \quad (5)$$

$$Q(t) = k_3 t^{1/2} + Q_0 \quad (6)$$

Here Q_e, Q(t) and Q_0 (mmol/g) are, respectively, the amounts of sorption at equilibrium, the time t and the saturated state, and k_1 (L/min), k_2 (g/(mmol min)) and k_3 (mmol/(min$^{1/2}$ g)) are the rate constants for pseudo first order, pseudo second order and intraparticle diffusion, respectively.

The resulting sorption rate constants are listed in Table 3. It is seen from Fig. 9 that the sorption of phosphate by C700 and MB by A800 occurred rapidly and approached saturation within a very short time. Phosphate sorption by A800 and G700 is clearly slower, proceeding gradually up to 24 h and becoming stable after longer reaction times. The correlation coefficients of Table 3 indicate that in all cases the pseudo-second order model fits the data better than the pseudo-first order model and the intraparticle diffusion model. The resulting phosphate sorption rate constants (k_2) for the various samples are clearly different, following the order G700 (0.004 g/(mmol min)) <A800 (0.053 g/(mmol min)) <C700 (6.6 g/(mmol min)). The formation of sample G by pelletizing powder sample C decreases the sorption rate by 10^3 orders. The Q_e values calculated from the pseudo-second order model are also in excellent agreement with the observed values, but those from the pseudo-first order model show differences. The MB sorption rate by sample A also shows better correlation with the pseudo-second order model than with the pseudo-first order model but an equally good correlation is obtained with the intraparticle diffusion model. Although the k_2 value for MB adsorption by sample A800 is nearly 20 times larger than that of phosphate adsorption, this may be related to the difference in the initial concentrations.

Table 3
Kinetic data for sorption of phosphate and methylene blue by three samples

Kinetic model	Sample			
	C700 Phosphate[a] (1.00)[b]	G700 Phosphate[a] (0.45)[b]	A800 Phosphate[a] (1.00)[b]	A800 MB[a] (0.025)[b]
Pseudo-first order				
Q_e^{Cal}(mmol/g)	0.78	0.53	0.57	0.072
k_1 (L/min)	0.156	0.003	0.008	0.072
R^2	0.9687	0.9402	0.8515	0.9409
Pseudo-second order				
Q_e^{Cal}(mmol/g)	1.00	0.49	1.00	0.025
k_2 (g/(mmol min))	6.57	0.004	0.053	107
R^2	1.0000	0.9943	0.9999	0.9999
Intraparticle diffusion				
Q_e^{Cal}(mmol/g)	0.99	0.41	0.87	0.025
k_3 (mmol/(g min$^{0.5}$))	0.193	0.0012	0.105	0.0048
R^2	0.9361	0.9824	0.9014	0.9999

[a] Sorbate.
[b] Q_e^{Obs}(mmol/g).

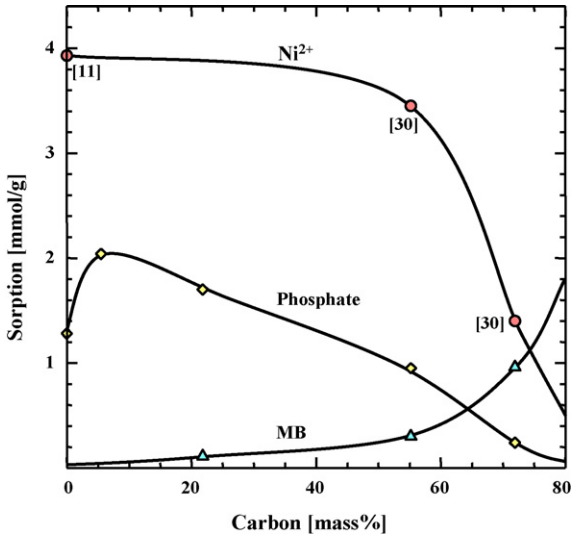

Fig. 10. Change of Ni^{2+}, phosphate and MB sorption by the present samples, CAS [11] and RPF [30] as a function of carbon content.

3.6. Comparison of sorption properties with RPF and CAS

We have previously reported the sorption abilities of CAS [11] and RPF [30], which differ from the present samples in their contents of CAS and activated carbon. Since RPF is consisted of used paper and plastics prepared for the purpose to get thermal energy by burning, it has higher carbon content than PS. It is therefore interesting to compare their sorption performance for Ni^{2+}, phosphate and MB. Fig. 10 shows these sorption capacities as a function of C content. In general, the sorption of Ni^{2+} and phosphate decreases while that of MB increases with increasing carbon content. A carbon content of 50–60 mass% appears to be optimum for simultaneous uptake of heavy metals (for example, Ni^{2+}), harmful oxyanions (for example, phosphate) and organic dyes (for example, MB).

4. Conclusion

Low cost, highly effective sorbents for removing harmful inorganic and organic cations and anions from water were prepared from paper sludge, which consists of organic fibers and inorganic fillers (kaolinite ($Al_2Si_2O_5(OH)_4$), calcite ($CaCO_3$) and talc ($Mg_3Si_4O_{10}(OH)_2$)), by grinding, calcining and/or physical activation of the paper sludge, with the following results:

(1) Heating the PS up to 800 °C decomposes the original inorganic phases and forms amorphous $CaO–Al_2O_3–SiO_2$ (CAS), which crystallizes to gehlenite ($Ca_2Al_2SiO_7$) and anorthite ($CaAl_2Si_2O_8$) at 900 °C. The organic fibers in the PS burn out upon heating in air, as in the calcined sample C and the ground pellet sample G, but is converted to activated carbon in the activated powder sample A which was prepared by physical activation of PS in wet N_2.
(2) The physically activated sample A shows relatively higher S_{BET} values (70 m^2/g at 600 °C) than the other samples. The S_{BET} value of sample G (37 m^2/g) is increased significantly by the mechanical activation which forms fine particles, but this parameter decreases steeply above 800 °C due to sintering.
(3) Qualitative sorption experiments indicate that maximum sorption of phosphate occurs in samples C and G heated at 700 °C, but in sample A heated at 800 °C.
(4) The sorption isotherms for phosphate and MB are fitted better by the Langmuir model than the Freundlich model. The saturation sorption capacities (Q_0) for phosphate were 2.04, 1.70 and 1.38 mmol/g in samples C700, A800 and G700, respectively. The Q_0 value for MB sorption by sample A800 was 0.11 mmol/g. The multi-sorption properties of sample A are attributed to the presence of amorphous CAS and activated carbon in the sample.
(5) The sorption kinetics of phosphate and MB are fitted best by the pseudo-second order model. The rate constants for phosphate sorption increase in the order G700 < A800 < C700.
(6) The sample with a carbon content of 50–60 mass% are suggested to be optimum for simultaneous uptake of heavy metals (for example, Ni^{2+}), harmful oxyanions (for example, phosphate) and organic dyes (for example, MB).

Acknowledgements

MH would like to express his gratitude to UNESCO/MEXT, Japan for the award of a research fellowship. The authors are grateful to Professor K.J.D. MacKenzie of Victoria University of Wellington for critical reading and editing of the manuscript.

References

[1] C.L. Henry, Nitrogen dynamics of pulp and paper sludge amendment to forest soils, Water Sci. Tech. 24 (1991) 417–423.
[2] R.R. Tripepi, X. Zhang, A.G. Campbell, Use of raw and composted paper sludge as a soil additive or mulch for cottonwood plants, Comp. Sci. Util. 4 (1996) 26–30.
[3] J. Tay, K. Show, Utilization of municipal wastewater sludge as building and construction material, Resour. Conserv. Recycl. 6 (1992) 191–204.
[4] B. Ahmadi, W. Al-Khaja, Utilization of paper waste sludge in the building construction industry, Resour. Conserv. Recycl. 32 (2001) 105–113.
[5] J. Pera, A. Amrouz, Development of highly reactive metakaolin from paper sludge, Adv. Cement Based Mater. 7 (1998) 49–56.
[6] T. Wajima, M. Haga, K. Kuzawa, H. Ishimoto, O. Tamada, K. Ito, T. Nishiyama, R.T. Downs, J.F. Rakovan, Zeolite synthesis from paper sludge ash at low temperature (90 °C) with addition of diatomite, J. Hazard. Mater. 132 (2006) 244–252.
[7] K. Hiyoshi, Sh. Muramatsu, M. Saito, Use of paper sludge ash as paper filler and pigment, Kami Pa Gikyoshi/Japan Tappi J. 59 (2005) 69–77.
[8] J. Son, H.-S. Yang, H.J. Kim, Physico-mechanical properties of paper sludge-thermoplastic polymer composites, J. Therm. Comp. Mater. 17 (2004) 509–522.
[9] T. Toya, Y. Kameshima, A. Nakajima, K. Okada, Preparation and properties of glass-ceramics from kaolin clay refining waste (Kira) and paper sludge ash, Ceram. Int. 32 (2006) 789–796.
[10] N.R. Khalili, M. Campbella, G. Sandi, J. Golaś, Production of micro- and mesoporous activated carbon from paper mill sludge. I. Effect of zinc chloride activation, Carbon 38 (2000) 1905–1915.
[11] V.K. Jha, Y. Kameshima, A. Nakajima, K. Okada, K.J.D. MacKenzie, Multifunctional uptake behaviour of materials prepared by calcining waste paper sludge, J. Environ. Sci. Health A41 (2006) 703–719.

[12] K. Okada, Y. Ono, Y. Kameshima, A. Nakajima, K.J.D. MacKenzie, Simultaneous uptake of ammonium and phosphate ions by compounds prepared from paper sludge ash, J. Hazard. Mater. B141 (2007) 622–629.
[13] Annual Book of ASTM Standards Volume 15.02: Glass, Ceramic Whitewares, 2001, pp. 118–119.
[14] Annual Book of ASTM Standards Volume 15.02: Glass, Ceramic Whitewares. 2001. 95–96.
[15] K. Okada, N. Yamamoto, Y. Kameshima, A. Yasumori, Porous properties of activated carbon from waste newspaper prepared by chemical and physical activation, J. Colloid Interface Sci. 262 (2003) 179–193.
[16] J. Temuujin, K. Okada, Ts. Jadambaa, K.J.D. MacKenzie, J. Amarsanaa, Effect of grinding on preparation of porous material from talc by selective leaching, J. Mater. Sci. Lett. 21 (2002) 1607–1609.
[17] K. Kubo, Mechanochemistry of Inorganic Materials, Sogo-Gijutsu Press, Tokyo, 1987.
[18] V.K. Jha, Y. Kameshima, K. Okada, K.J.D. MacKenzie, Ni^{2+} uptake by amorphous and crystalline $CaAl_2SiO_7$ synthesized by solid-state reaction of kaolinite, Sep. Purif. Tech. 40 (2004) 209–215.
[19] J. Temuujin, K. Okada, K.J.D. MacKenzie, Preparation of porous silica from vermiculite by selective leaching, Appl. Clay Sci. 22 (2003) 187–195.
[20] M. Shimada, T. Iida, K. Kawarada, Pore structure and adsorption properties of activated carbon prepared from granular molded waste paper, J. Mater. Cycles Waste Manage. (2004) 111–118.
[21] R. Chitrakar, S. Tezuka, A. Sonoda, K. Sakane, K. Ooi, T. Hirotsu, Adsorption of phosphate from seawater on calcined Mg-Mn-layered double hydroxides, J. Colloid Interface Sci. 290 (2005) 45–51.
[22] A. Drizo, Ch. Forget, R.P. Chapuis, Y. Comeau, Phosphorus removal by electric arc furnace steel slag and serpentine, Water Res. 40 (2006) 1547–1554.
[23] B. Kostura, H. Kulveitová, J. Leško, Blast furnace slags as sorbents of phosphate from water solutions, Water Res. 39 (2005) 1795–1802.
[24] S. Kaneko, K. Nakajima, Phosphorus removal by crystallization using a granular activated magnesia clinker, J. Water Pollut. Control Fed. 60 (1988) 1239–1244.
[25] W. Xie, Q. Wang, H. Ma, H. Ogawa, Phosphate removal from wastewater using aluminum oxide as adsorbent, Int. J. Environ. Pollut. 23 (2005) 486–491.
[26] M. Özacar, A. Şengil, Enhancing phosphate removal from wastewater by using polyelectrolytes and clay injection, J. Hazard. Mater. B100 (2003) 131–146.
[27] K. Okada, J. Temuujin, Y. Kameshima, K.J.D. MacKenzie, Simultaneous uptake of ammonium and phosphate ions by composites of g-alumina/potassium aluminosilicate gel, Mater. Res. Bull. 38 (2003) 749–756.
[28] I.J. Langmuir, The adsorption of gases on plane surfaces of glass, mica and platinum, J. Am. Chem. Soc. 40 (1918) 1361–1403.
[29] H. Freundlich, W. Heller, The adsorption of *cis*- and *trans*-azobenzene, J. Am. Chem. Soc. 61 (1939) 2228–2230.
[30] Z. Kadirova, Y. Kameshima, A. Nakajima, K. Okada, Preparation and sorption properties of porous materials from refuse paper and plastic fuel (RPF), J. Hazard. Mater. B 137 (2006) 352–358.
[31] T.L. Eberhardt, S.-H. Min, J.S. Han, Phosphate removal by refined aspen wood fiber treated with carboxymethyl cellulose and ferrous chloride, Bioresour. Tech. 97 (2006) 2371–2376.
[32] H. Ye, F. Chen, Y. Sheng, G. Sheng, J. Fu, Adsorption of phosphate from aqueous solution onto modified palygorskites, Sep. Purif. Tech. 50 (2006) 283–290.
[33] F. Banat, S. Al-Asheh, L. Al-Makhadmeh, Evaluation of the use of raw and activated date pits as potential adsorbents for dye containing waters, Process Biochem. 39 (2003) 193–202.
[34] N. Kannan, M.M. Sundaram, Kinetics and mechanism of removal of methylene blue by adsorption on various carbons-a comparative study, Dyes Pigments 51 (2001) 25–40.
[35] S. Karaca, A. Gürses, R. Bayrak, Effect of some pretreatments on the adsorption of methylene blue by Balkaya lignite, Energy Convers. Manage. 45 (2004) 1693–1704.
[36] A. Gürses, S. Karaca, C. Dogar, R. Bayrak, M. Acikyildiz, M. Yalcin, Determination of adsorptive properties of clay/water system: methylene blue sorption, J. Colloid Interface Sci. 269 (2004) 310–314.
[37] C.D. Woolard, J. Strong, C.R. Erasmus, Evaluation of the use of modified coal ash as a potential sorbent for organic waste streams, Appl. Geochem. 17 (2002) 1159–1164.
[38] R.L. Tseng, F.C. Wu, R.S. Juang, Liquid-phase adsorption of dyes and phenols using pinewood-based activated carbons, Carbon 41 (2003) 487–495.
[39] K. Okada, N. Yamamoto, Y. Kameshima, A. Yasumori, Adsorption properties of activated carbon from waste newspaper prepared by chemical and physical activation, J. Colloid Interface Sci. 262 (2003) 194–199.
[40] S. Lagergren, B.R. Svenska, Zur theorie der sogenannten adsorption geloester stoffe, Veternkapsakad Handlinger 24 (1898) 1–39.
[41] Y.S. Ho, D.A.J. Wase, C.F. Forster, Kinetic studies of competitive heavy metal adsorption by sphagnum moss peat, Environ. Tech. 17 (1996) 71–77.
[42] G. McKay, M.S. Otterburn, A.G. Sweeney, The removal of colour from effluent using various adsorbents-III. Silica: rate processes, Water Res. 14 (1980) 15–20.